Thermodynamic Properties for the Solid−Liquid Phase Transition of Silybin + Poloxamer 188

Wei Han,[†] TongChun Bai,*[,†] and Jian-Jun Zhu[‡]

College of Chemistry, Chemical Engineering and Materials Science, Soochow University, Suzhou, 215123, China, and Department of Chemistry, State University of New York, Stony Brook, New York 11796

Mixtures of silybin (1) + poloxamer 188 (2) were prepared by a method of fusion cooling. Temperature (T_{fus}) and enthalpy of fusion ($\Delta_{fus}H$) versus mass fraction of silybin were measured by a DSC method. A eutectic point with $w_1 = 0.25$ and $T_{fus,E} = 325.4$ K was observed. IR spectroscopy and X-ray powder diffraction results indicate that the spectra of mixtures can be regarded as the superposition of those of pure silybin and poloxamer 188. There was no significant change in the crystal structure of silybin and poloxamer in the mixed solid. The experimental T_{fus}, w_1 diagram was fitted by using the Flory−Huggins model with a fair agreement.

Introduction

Drugs are mainly hydrophobic organic compounds. The solubility and dissolution rate of biologically active compounds are often limiting factors for their applicability. Therefore, the study of bioavailability of drugs and their solubility/dissolution enhancement are important tasks in pharmaceutical technology.[1,2] Among the techniques of increasing the rate of drug dissolution, the solid dispersion method is one of the most popular.[3−8] However, there are still some problems limiting the application of solid dispersions. For example, the preparation method by fusion at higher temperature usually causes drug decomposition. An optimum carrier not only spreads drug uniformly but also decreases the melting temperature of the formulation. Therefore, data on enthalpy of fusion and the phase diagram of solid−liquid equilibrium for solid dispersions are required.

Silymarin is a mixture of flavonolignans extracted from the seeds of milk thistle, *Silybum marianum*.[9] The major component of silymarin is silybin, which constitutes (60 to 70) % of the drug.[10−12] The molecular structure of silybin is shown in Figure 1. Possibly due to its antioxidant and membrane stabilizing properties, the compound has been shown to protect different organs and cells against a number of harmful organisms. Its use has been widespread since preparations became officially available for clinical use.[13−15] A major problem in the development of an oral solid dosage form of this drug is the extremely poor aqueous solubility, possibly resulting in dissolution-limited oral absorption.[16]

Poloxamer 188 (P188) is a water-soluble, nonionic, triblock copolymeric surfactant consisting of a hydrophobic center chain (block) of polyoxypropylene oxide with two long hydrophilic chains (blocks) of polyoxyethylene oxide (see Figure 2). The average molecular weight of P188 is 8400 Da.[17] Poloxamer 188 has been used extensively in pharmacological and physiological studies. It has been demonstrated that P188 is associated with a significant capacity to facilitate repair of damaged membranes.[18] Research results also indicate that poloxamers are efficient as additives to suppress aggregation and to facilitate refolding of denatured proteins in solution.[19] Poloxamers have been included in liposomal drug delivery systems, to sterically stabilize liposome and to prolong the duration of their circulation in the bloodstream.[20,21]

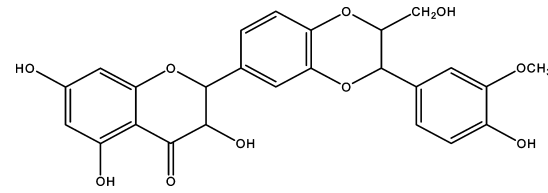

Figure 1. Chemical structure of silybin, 3,5,7-trihydroxy-2-[3-(4-hydroxy-3-methoxyphenyl)-2-hydroxymethyl-2,3-dihydrobenzo-[1,4] dioxin-6-yl]-chroman-4-one.

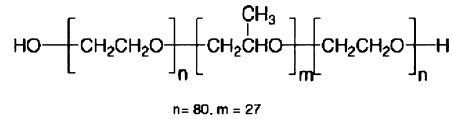

Figure 2. Chemical structure of poloxamer 188.

Polymers, such as polyethylene glycol (PEG) and polyvinylpyrrolidone (PVP), have frequently been used as carriers in solid dispersion formulations.[4,5,8] In this work, the thermodynamic properties of the mixture of silybin + poloxamer 188 were determined. One interest is the study on the possible effect of poloxamer 188 on reducing the melting temperature of silybin + P188 solid dispersions. The melting temperature (T_{fus}) and the enthalpy of fusion, $\Delta_{fus}H$, were measured by differential scanning calorimetry (DSC). The phase diagram and the enthalpy diagram were constructed from experimental data. The data were fitted to the Flory−Huggins model. FT-IR spectroscopy and powder X-ray diffraction were performed to elucidate the structure and possible drug-carrier interactions.

Experimental Section

Materials. Silybin (CAS Registry No.: 22888-70-6) was purchased from Panjin Green Biological Development Co. Ltd., Liaoning, China. Its purity was claimed to be 97 % by UV spectrometry at (252 to 288) nm. This purity was confirmed by

* Corresponding author. E-mail: tcbai@suda.edu.cn. Tel.: +(86)51265880363. Fax: +(86)51265880089.
[†] Soochow University.
[‡] State University of New York.

10.1021/je900051w CCC: $40.75
Published on Web 04/06/2009

our HPLC measurement with 96.8 % silybin, 1.1 % isosilybin, 0.8 % silydianin, 0.1 % silychristin, and 1.2 % other impurities. Before experiment, the drug was dried under vacuum at 353 K over 24 h. Poloxamer 188, chemical agent, was received from ICN Biomedicals Inc., USA. Both reagents were stored over P_2O_5 in a desiccator before use.

Preparation of Samples. Silybin and poloxamer 188 were accurately weighted, mixed, and ground in an agate mortar for more than 1 h. This mixture was heated and stirred in a glass container in a water bath at 353 K and then rapidly cooled in liquid nitrogen (flash cooling) for more than 30 min. Subsequently, the mixture was ground, heated, stirred, and cooled three times. Then the sample was stored over P_2O_5 in a desiccator for more than 72 h until use. A trace amount of other compositions coexisted with silybin and had little influence on silybin's medicinal efficiency because of their similar structures.[10−12] Therefore, the system is treated as a pseudo binary mixture composed of silybin and poloxamer 188. Samples composed of different content ratios were prepared.

Differential Scanning Calorimeter (DSC). DSC measurements were carried out with a differential scanning calorimeter (NETSCH, DSC-204F1, Germany). A certified indium wire encapsulated in an aluminum crucible (supplied by the instrument manufacturer) was used for temperature and heat flow calibration. An aluminum pan and lid with a pinhole were used to contain the sample. An empty container of the same type was employed as a reference. Nitrogen gas of 99.999 % purity was used as purge gas, at a rate of 20 mL·min^{-1}, and protective gas, 70 mL·min^{-1}, for DSC operation. Samples (about 5 mg) were weighed to ± 0.01 mg using a balance (model: BT25S, SARTORIUS AG, Beijing). A mass loss profile of pure silybin solid was measured by TG, PE-DELTA SERIES 7, with a N_2 flow rate of 20 mL·min^{-1}. The TG curve shows that silybin decomposes above 473 K. In DSC measurements, samples were heated at a rate of 5 K·min^{-1}, over a temperature range from (288 to 453) K. The temperatures of peak top, T_{top}, peak onset, T_{onset}, and the enthalpy of fusion, $\Delta_{fus}H$, were determined by using the software of NETZSCH Proteus. All samples were measured in triplicate. The uncertainties of experiments are estimated to be ± 0.1 K for the temperature, 0.1 % for the heat of fusion, and 0.002 for mass fraction.

To describe with accuracy the heat transfer during the melting process, it is desirable to use the lower heating rate.[22] However, after the eutectic composition, the melting process of silybin took place. The lower the scanning rate, the broader the melting peak becomes, and the more difficult the determination of peak onset point becomes. This leads to a greater error for the calculation of peak area and peak onset point. To overcome this difficulty, a scanning rate of 5 K·min^{-1} is used. This value is lower than the rate commonly used in DSC operation, 10 K·min^{-1}, and higher than the minimum operation, 1 K·min^{-1}.

Infrared Spectroscopy. Fourier transform-infrared (FT-IR) spectra were obtained on a Magna 550 FT-IR system (Nicolet, USA) with the KBr disk method. The scanning range was (400 to 4000) cm^{-1}, and the resolution was 2 cm^{-1}.

X-ray Powder Diffraction. Powder X-ray diffraction investigations were performed with a diffractometer (model: X'PERT PRO MPD, PANalytical Company, Holland): Cu Kα, λ = 0.15406 nm, voltage: 40 kV, and 40 mA, with the angular range of $(3 < 2\theta < 60)°$ in a step scan mode (step width 0.03).

Results and Discussions

DSC Tracings. DSC measurement was performed on samples of silybin (1) + poloxamer 188 (2) with different compositions.

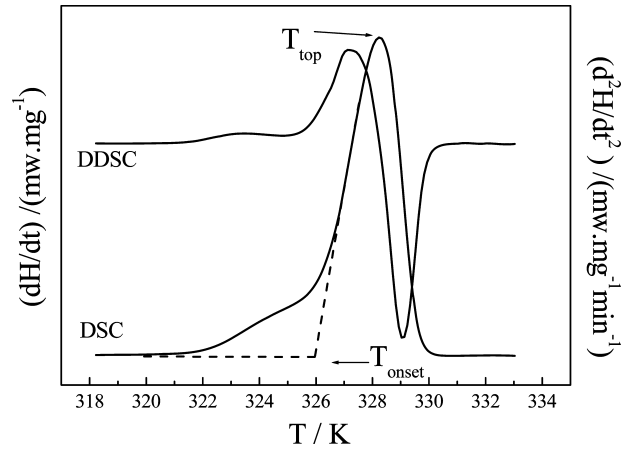

Figure 3. DSC tracing and its first differential curves (DDSC) of poloxamer 188. T_{onset} is the temperature at peak onset, and T_{top} is the temperature at the peak top.

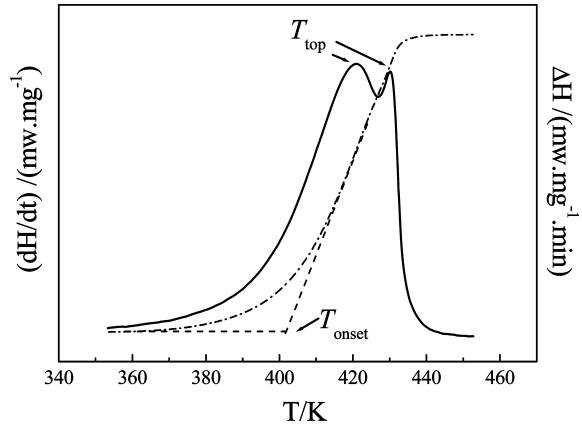

Figure 4. DSC profile (solid line) and its integral (dash dot line) for the process of fusion of silybin. T_{onset} is the temperature at the integral onset point, and T_{top} is the temperature at peak top of DSC.

As shown in Figure 3, poloxamer 188 displays a melting endotherm with a shoulder at the lower side, which indicates the presence of more than one crystal form of poloxamer. This transition can be clearly shown from its first differential curve, DDSC, where a plateau region can be seen before the melting process. As in the case of PEG 6000,[5,6] this transition corresponds to the defolding of a once folded form. The temperature of the onset point corresponding to the fusion of poloxamer 188, T_{onset}, is 326.0 K. The enthalpy of fusion is 146 J·g^{-1}, which can be obtained by the software of NETZSCH analytical Proteus

The profile of silybin is shown in Figure 4. For samples used in this work, the melting peak was split into two peaks, which correspond to two geometric isomers (silybin A and B[11,12]). The temperatures of two peak tops are (421.1 and 429.8) K, respectively. The total enthalpy of fusion is 161 J·g^{-1}. The temperature of peak onset, T_{onset}, can be calculated by the software of NETZSCH analytical Proteus. For mixtures of silybin + poloxamer 188, as shown in Figure 5, the phenomenon of peak splitting for the silybin fusion process disappears, and the more poloxamer that is mixed, the broader the peak becomes. For these systems, it is difficult to distinguish the baseline and the peak onset. Therefore, the determination of the peak onset by the extrapolating method, exploring the tangential line from the inflection point to cross the baseline, is in considerable error. However, if we construct the integral DSC curve, the onset point can be clearly shown. Comparing the results of two methods to

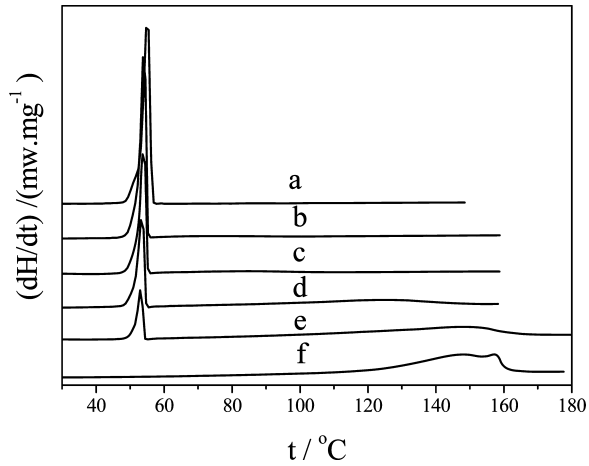

Figure 5. DSC profiles of mixtures of silybin (1) + poloxamer 188 (2). From top to bottom: w_1 = a, 0; b, 0.168; c, 0.250; d, 0.500; e, 0.800; and f, 1.0.

Table 1. Temperatures at Peak Onset (T_{onset}/K), Peak Top (T_{top}/K), and the Enthalpies of Fusion ($\Delta_{fus}H$/J·g^{-1}) for Mixtures of Silybin (1) + Poloxamer 188 (2)

	peak 1			peak 2		
100 w_1	T_{onset}/K	T_{top}/K	$\Delta_{fus}H(1)$/J·g^{-1}	T_{onset}/K	T_{top}/K	$\Delta_{fus}H(2)$/J·g^{-1}
0	326	328.3	146			
4.0	325.8	328.2	130			
8.0	325.6	327.9	124			
12.0	325.6	327.9	123			
16.7	325.5	327.3	117			
17.5	325.2	327.3	115			
20.0	325.2	327.3	112			
22.2	325.1	327.3	110			
25.0	325.4	327.3	110			
33.3	325	326.9	99.1	346.7	365.7	15.0
40.0	325	327	83.0	355.3	375.4	38.8
50.0	324.5	327	74.0	362.8	389.1	65.5
60.0	324.7	326.9	68.3	370.7	396.3	79.7
70.0	324.4	326.5	44.9	377.8	404.6	120
80.0	324.4	326.4	30.8	387.3	421.4	146
90.0	324.2	326.1	12.1	398.6	426.8	171
100				402.5	421.1	161
					429.8	

the peak of silybin, it shows that the onset temperature of the integral curve is slightly higher than the DSC curve. However, this difference is smaller than the error obtained directly from the DSC curve, especially for those cases of lower scanning rate and x_1. Therefore, for the fusion peak of silybin, the onset point was determined from their integral. The temperature of integral onset T_{onset} was used to determine the temperature of fusion.

For samples of silybin (1) + P188 (2) with the composition $w_1 < 0.25$, the DSC profiles show the absence of the peak of silybin fusion (Figure 5a, b, and c). This result suggests that silybin was completely dissolved in the liquid phase. Because the melting temperatures of the eutectic composition and poloxamer 188 overlap at this region, DSC profiles are the combination of two melting processes. With the increase in w_1, the second endothermic peak corresponding to the drug fusion gradually appears and shifts toward the melting temperature of pure silybin (curves d, e, and f). The higher the w_2, the more broad the peak becomes. Some parameters of the DSC curve, T_{onset}, T_{top}, and $\Delta_{fus}H$, are listed in Table 1.

Phase Diagram. The phase diagram of silybin and poloxamer 188 is presented in Figure 6, in which the temperature of onset for DSC peak 1 and the temperature of onset for the integral of peak 2 are used to express the fusion temperatures. A eutectic

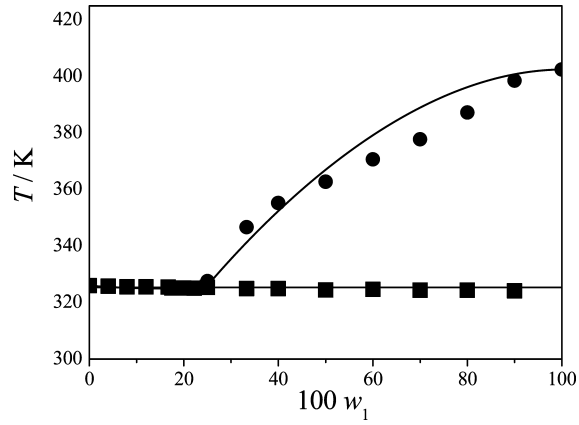

Figure 6. Phase diagram for mixtures of silybin (1) + poloxamer 188 (2). The temperature of peak onset for DSC peak 1 is expressed by ■, and the temperature of onset for peak 2 is expressed by ●. A eutectic point is found at $w_1 = 0.250$, $T_{fus} = 325.4$ K.

point is found at $w_{1,E} = 0.250$, $T_{fus,E} = 325.4$ K with $\Delta_{fus}H = 110$ J·g^{-1}. Below the eutectic composition, the phase diagram can be considered as a special type, where the liquidus and the solidus curves are superposed. Similar phase diagrams have been observed in silybin + PEG 6000 and other drug systems.[2,3]

To fit the freezing curves, equilibrium between a pure solid phase and a liquid mixture is assumed. Neglecting the influence of the heat capacities as well as of pressure, the solubility of a component i at atmospheric pressure can be expressed as[23]

$$\ln x_i\gamma_i = \frac{-\Delta_{fus}H_{m,i}^*}{RT}\left(1 - \frac{T_{fus}}{T_{fus,i}^*}\right) \quad (1)$$

Here, x_i represents the mole fraction of substance i in the liquid phase. $\Delta_{fus}H_{m,i}^*$ and $T_{fus,i}^*$ are the molar enthalpy and temperature of fusion of pure component i, respectively. The Flory−Huggins model was used to calculate the activity coefficient γ_i[23]

$$\ln \gamma_1 = \ln[\phi_1/x_1] + (1 - V_{m,1}/V_{m,2})\phi_2 + \phi_2^2\chi/RT \quad (2)$$

In the silybin-rich region, where w_1 changes from eutectic composition to $w_1 = 1$, we have

$$T_f = \frac{\Delta_{fus}H_{m,1}^* + \chi\phi_2^2}{\Delta_{fus}H_{m,1}^*/T_{fus,1}^* - R[\ln \phi_1 + \phi_2(1 - V_{m,1}/V_{m,2})]} \quad (3)$$

where χ is a theoretical interaction parameter. The volume fraction ϕ_i was calculated by the van der Waals volume V_{vdw}. The van der Waals volume was calculated by the group-contribution method as described by Bondi.[24]

$$\phi_i = \frac{(w_i/M_i)V_{vdwi}}{(w_1/M_1)V_{vdw1} + (w_2/M_2)V_{vdw2}} \quad (4)$$

in which M_i is the mole mass of substance i. Because the liquidus curve and the three-phases curve are superposed in the region rich in poloxamer 188, theoretical fitting was performed only in the silybin-rich region. By a nonlinear least-squares method, parameter χ was obtained. The fitting result is shown in Figure 6 in a line, and some relative parameters are listed in Table 2.

Enthalpy of Fusion. Figure 7 shows the difference of the enthalpy of fusion, $\delta_{fus}H$, as defined in eq 5.

$$\delta_{fus}H = \Delta_{fus}H(12) - [w_1\Delta_{fus}H(1) + (1 - w_1)\Delta_{fus}H(2)] \quad (5)$$

where $\Delta_{fus}H(12)$ is the sum of peak 1 and 2 and $\Delta_{fus}H(1)$ and $\Delta_{fus}H(2)$ are the enthalpy of fusion of pure silybin and

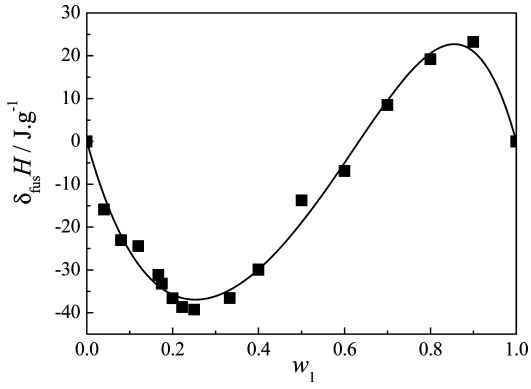

Figure 7. Difference of the enthalpy of fusion, $\delta_{fus}H$, for mixtures of silybin (1) + poloxamer 188 (2), where points ■ are experimental data and the line is the R−K equation fit.

Table 2. Parameters of Phase Diagram $T-w_1$

	silybin	poloxamer 188
M/g·mol^{-1}	482.12	8400
segment number		n:m = 80:27
V_{vdw}/cm^3·mol^{-1}	230.48	4655.3
T_{fus}*/K	402.5	326.0
$\Delta_{fus}H$*/J·g^{-1}	161	146
χ/J·mol^{-1}		−21000
eutectic composition, $w_{1,E}$		0.250
temperature of eutectic point $T_{fus,E}$/K		325.4

Table 3. Parameters of the Redlich−Kister Equation for Fitting $\delta_{fus}H$/J·g^{-1}, the Standard Error σ, and the Regression Coefficient r

H_0	H_1	H_2	H_3	σ	r
−360	845	−985	866	2.6	0.993

poloxamer (in J·g^{-1}), respectively. It was shown in Figure 7 that a negative minimum is observed at $w_1 = 0.25$, which corresponds to the eutectic composition in Figure 6. It suggests that the formation of eutectic composition is energy favorable. However, in the region rich in silybin, a positive maximum is observed, which corresponds to an energy unfavorable mixing. The Redlich−Kister (R−K) equation[23] was used to fit $\delta_{fus}H$.

$$\delta_{fus}H = w_1 w_2 \sum_{v=0}^{3} H_v (w_1 - w_2)^v \qquad (6)$$

Parameters of eq 6 are shown in Table 3.

FT-IR Spectroscopy. To further study the possibility of an interaction between silybin and poloxamer 188, more information was gathered using FT-IR spectroscopy. The possible interaction could occur between the −O− group of poloxamer 188 and the −OH and C═O groups of silybin. Any interaction would be reflected by shifts in −OH, −O−, and C═O vibration. The infrared spectra of silybin, poloxamer 188, and some of their mixtures are shown in Figure 8.

For silybin, the band at 3453 cm^{-1} is assigned to free −OH bond vibration, whereas 3175 cm^{-1} is assigned to −OH bond vibration connected with group interaction; 1644 cm^{-1} is assigned to the stretching vibration of the band of C═O group; 1514 cm^{-1} is assigned to the aromatic group; and 1170 cm^{-1} is assigned to C−O−C vibration.

For poloxamer 188, the band at 1111 cm^{-1} is assigned to the C−O−C group vibration; 2882 cm^{-1} is assigned to the CH_2 group vibration; and 3453 cm^{-1} is assigned to OH group vibration.

The spectra can be simply regarded as the superposition of those of silybin and poloxamer 188. In Figure 8, the absorption band at 3453 cm^{-1}, assigned to the free −OH, is present in all

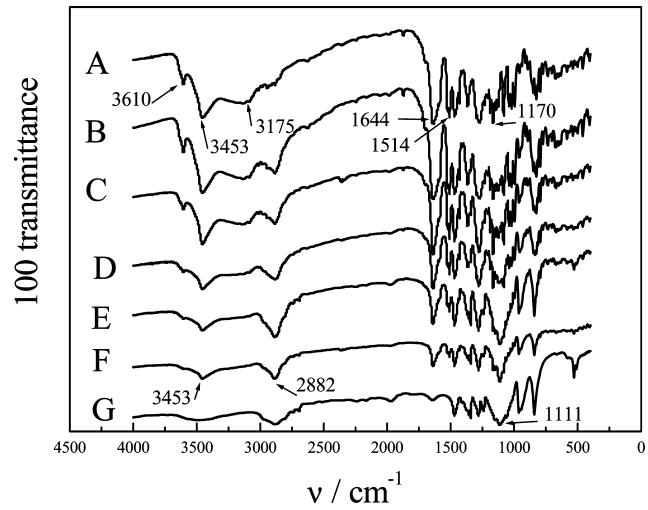

Figure 8. FT-IR spectra of solid mixtures of poloxamer 188 + silybin. Mass fraction of silybin w_1 = A, 1; B, 0.800; C, 0.600; D, 0.250; E, 0.200; F, 0.182; and G, 0.

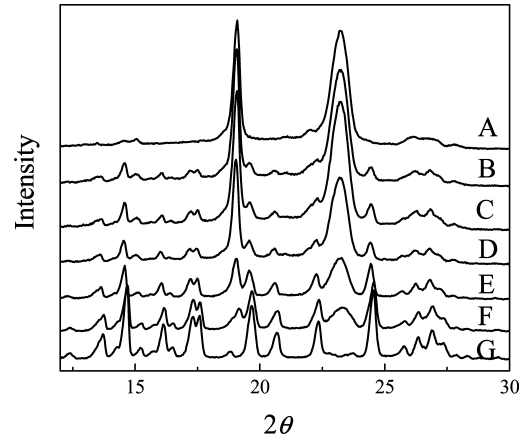

Figure 9. X-ray diffraction patterns for mixtures of poloxamer 188 + silybin. Mass fraction of silybin w_1 = A, 0; B, 0.167; C, 0.200; D, 0.250; E, 0.600; F, 0.800; and G, 1.0.

cases, but its intensity is reduced for samples of lower silybin content. However, the band assigned to OH due to intermolecular association at 3175 cm^{-1} is decreased in intensity in the sequence of w_1 = 1, 0.800, and 0.600. It indicates that the intramolecular hydrogen bond is present for the undispersed silybin. When silybin was dispersed into poloxamer, as in the cases of w_1 = 0.250, 0.200, and 0.182, the group interaction disappeared. No indication for hydrogen bonding between silybin and poloxamer 188 was observed at w_1 = 0.250, 0.200, and 0.182.

X-ray Diffraction. Figure 9 shows some examples of the X-ray diffraction pattern for silybin, poloxamer 188, and their mixtures. The characteristic peaks of poloxamer 188 shows two peaks with highest intensity at 2θ of 19.094° and 23.204°. Characteristic peaks of silybin at 14.649°, 24.542°, 19.662°, 17.590°, 17.323°, and 16.119° could be detected in the sequence of their relative intensity. These peaks could be detected in mixtures of silybin + poloxamer 188. Figure 9 suggests that the crystalline nature of silybin was still maintained. The relative reduction of diffraction intensity of silybin in poloxamer 188 suggests that the amount of drug in the samples is decreased. The positions of silybin patterns were the same in the mixtures, which ruled out the possibility of compound formation between poloxamer 188 and silybin.

Conclusion

A eutectic point with $w_{1,E} = 0.25$ and $T_{fus,E} = 325.4$ K was observed in silybin + poloxamer 188 mixtures. IR spectroscopy and X-ray diffraction results indicate that there are no significant changes in the crystal structures of silybin and poloxamer 188 in their mixtures. The fitted experimental T_{fus} and w_1 diagram is in fair agreement with the Flory−Huggins model.

Literature Cited

(1) Hörter, D.; Dressman, J. B. Influence of Physicochemical Properties on Dissolution of Drugs in the Gastrointestinal Tract. *Adv. Drug Delivery Rev.* **2001**, *46*, 75–87.

(2) Bai, T. C.; Yan, G. B.; Hu, J.; Zhang, H. L.; Huang, C. G. Solubility of silybin in aqueous poly(ethylene glycol) solution. *Int. J. Pharm.* **2006**, *308*, 100–106.

(3) Vasconcelos, T.; Sarmento, B.; Costa, P. Solid Dispersions as Strategy to Improve Oral Bioavailability of Poor Water Soluble Drugs. *Drug Discovery Today* **2007**, *12*, 1068–1075.

(4) Yao, W. W.; Bai, T. C.; Sun, J. P.; Zhu, C. W.; Hu, J.; Zhang, H. L. Thermodynamic Properties for the System of Silybin and Poly(ethylene glycol) 6000. *Thermochim. Acta* **2005**, *437*, 17–20.

(5) Naima, Z.; Siro, T.; Juan-Manuel, G. D.; Chantal, C.; René, C.; Jerome, D. Interactions Between Carbamazepine and Polyethylene Glycol (PEG) 6000: Characterisations of the Physical, Solid Dispersed and Eutectic Mixtures. *Eur. J. Pharm. Sci.* **2001**, *12*, 395–404.

(6) Damian, F.; Blaton, N.; Naesens, L.; Balzarini, J.; Kinget, R.; Augustijns, P.; Van den Mooter, G. Physicochemical Characterization of Solid Dispersions of the Antiviral Agent UC-781 with Polyethylene Glycol 6000 and Gelucire 44/14. *Eur. J. Pharm. Sci.* **2000**, *10*, 311–322.

(7) Verheyen, S.; Augustijins, P.; Kinget, R.; Van den Mooter, G. Melting Behavior of Pure Polyethylene Glycol 6000 and Polyethylene Glycol 6000 in Solid Dispersions Containing Diazepam or Temazepam: a DSC Study. *Thermochim. Acta* **2001**, *380*, 153–164.

(8) Van den Mooter, G.; Augustijins, P.; Blaton, N.; Kinget, R. Physicochemical Characterization of Solid Dispersions of Temazepam with Polyethylene Glycol 6000 and PVP K30. *Int. J. Pharm.* **1998**, *164*, 67–80.

(9) Wagner, H.; Selingman, O.; Lotter, H. *Flavonoids and Bioflavonoids*; Elsevier: Amsterdam, 1986.

(10) Lee, D. Y.-W.; Liu, Y. Molecular Structure and Stereochemistry of Silybin A, Silybin B, Isosilybin A, and Isosilybin B, Isolated from Silybum marianum (Milk Thistle). *J. Nat. Prod.* **2003**, *66*, 1171−1174.

(11) Lee, J. I.; Narayan, M.; Barrett, J. S. Analysis and Comparison of Active Constituents in Commercial Standardized Silymarin Extracts by Liquid Chromatography- Electrospray Ionization Mass Spectrometry. *J. Chromatogr. B* **2007**, *845*, 95–103.

(12) Kvasnicka, F.; Bíba, B.; Ševčík, R.; Voldřich, M.; Krátká, J. Analysis of the Active Components of Silymarin. *J. Chromatogr. A* **2003**, *990*, 239–245.

(13) Gažak, R.; Walterová, D.; Křen, V. Silybin and Silymarins - New and Emerging Applications in Medicine. *Curr. Med. Chem.* **2007**, *14*, 315.

(14) Wellington, K.; Jarvis, B. Silymarin: A Review of Its Clinical Properties in the Management of Hepatic Disorders. *Biodrugs* **2001**, *15*, 465–489.

(15) Saller, R.; Meier, R.; Brignoli, R. The Use of Silymarin in the Treatment of Liver Diseases. *Drugs* **2001**, *61*, 2035–2063.

(16) El-Samaligy, M. S.; Afifi, N. N.; Mahmoud, E. A. Increasing Bioavailability of Silymarin Using A Buccal Liposomal Delivery System: Preparation and Experimental Design Investigation. *Int. J. Pharm.* **2006**, *308*, 140–148.

(17) Nair, L. M.; Konkel, J.; Thomas, M.; Koberda, M. Comparison of Electrospray Ionization Mass Spectrometry and Evaporative Light Scattering Detections for the Determination of Poloxamer 188 in Itraconazole Injectable Formulation. *J. Pharm. Biomed. Anal.* **2006**, *41*, 725–730.

(18) Harting, M. T.; Jimenez, F.; Kozar, R. A.; Moore, F. A.; Mercer, D. W.; Hunter, R. L.; Cox, C. S.; Gonzalez, E. A. Effects of Poloxamer 188 on Human PMN Cells. *Surgery* **2008**, *144*, 198–203.

(19) Mustafi, D.; Smith, C. M.; Makinen, M. W.; Lee, R. C. Multi-block Poloxamer Surfactants Suppress Aggregation of Denatured Proteins. *Biochim. Biophys. Acta* **2008**, *1780*, 7–15.

(20) Woodle, M. C.; Newman, M. S.; Martin, F. J. Liposome Leakage and Blood Circulation: Comparison of Adsorbed Block Copolymers with Covalent Attachment of PEG. *Int. J. Pharm.* **1992**, *88*, 327–334.

(21) Castile, J. D.; Taylor, K. M. G.; Buckton, G. The Influence of Incubation Temperature and Surfactant Concentration on the Interaction between Dimyristoylphosphatidylcholine Liposomes and Poloxamer Surfactants. *Int. J. Pharm.* **2001**, *221*, 197–209.

(22) Jamil, A.; Kousksou, T.; Zeraouli, Y.; Dumas, J.-P. Liquidus Temperatures Determination of the Dispersed Binary System. *Thermochim. Acta* **2008**, *471*, 1–6.

(23) Acree, W. E. *Thermodynamic Properties of Nonelectrolyte Solutions*; Academic Press Inc.: 1984.

(24) Bondi, A. van der Waals Volumes and Radii. *J. Phys. Chem.* **1964**, *68*, 441–451.

Received for review January 14, 2009. Accepted March 11, 2009.

JE900051W